ELSEVIER

Materials Science and Engineering A354 (2003) 377–386

MATERIALS SCIENCE & ENGINEERING A

www.elsevier.com/locate/msea

Phase transition in a Cu–14.1Al–9.0Ni alloy

C.H. Chen *, C.C. Yang, T.F. Liu

Department of Materials Science and Engineering, National Chiao Tung University, Hsinchu 300, Taiwan, ROC

Received 1 May 2002; received in revised form 6 January 2003; accepted 7 January 2003

Abstract

The phase transition of the Cu–14.1 wt.% Al–9.0 wt.% Ni alloy has been examined by transmission electron microscopy and energy-dispersive X-ray analysis. In the as-quenched condition, the microstructure of the alloy was $D0_3$ phase that contained extremely fine L-J precipitates. During the early stage of isothermal aging at 500 °C, a high density of the extremely fine B2 particles was observed within the extremely thin lamellar γ_1' martensite, which was formed by a $D0_3 \rightarrow \gamma_1'$ martensitic transformation during quenching. With increasing aging time at 500 °C, the isothermal phase transition sequence was found to be $D0_3 \rightarrow D0_3 + B2 \rightarrow D0_3 + B2 + \alpha \rightarrow B2 + \alpha + \gamma_2$. This transition significantly differs from that observed by other researchers. Besides, both Kurdjumov–Sachs (K–S) and Nishiyama–Wassermann (N–W) orientation relationships between the B2 particle and the α phase could be detected in the aged alloy.

Keywords: Phase transition; Cu–Al–Ni alloy; Microstructure; SEM; TEM

1. Introduction

The effects of adding nickel on the microstructural changes of Cu–Al binary alloys have been extensively studied [1–13]. According to those studies, when an alloy with a chemical composition of Cu–(14–15.1) wt.% Al–(3.1–4.3) wt.% Ni was solution heat-treated at a point in the single β phase (disordered body-centered cubic) region and then quenched into room-temperature water or iced-brine, the microstructure was single $D0_3$ phase [1–4], or $D0_3$ phase that contained extremely fine 2H-type precipitates [5,6]. When the as-quenched alloy was aged at temperatures between 325 °C and 500 °C for a moderate duration and then quenched, γ_2 (Cu_9Al_4) particles firstly precipitated within the $D0_3$ matrix at the aging temperature, and the remaining $D0_3$ matrix was then transformed to γ_1' martensite during quenching [4,7,8]. Singh et al. claimed that, after the aging time at 500 or 550 °C was increased, the γ_2 particle grew and coalesced, and the remaining $D0_3$ matrix was completely transformed to a mixture of (α+β) phases at the aging temperature [7–9]. Consequently, the phase transition sequence at 500 or 550 °C was $D0_3 \rightarrow D0_3 + \gamma_2 \rightarrow \gamma_2 + \alpha + \beta$. Besides, Singh et al. also found that the γ_2 particle decomposed into B2 (NiAl) phase after aged at 500 °C for a long period [8].

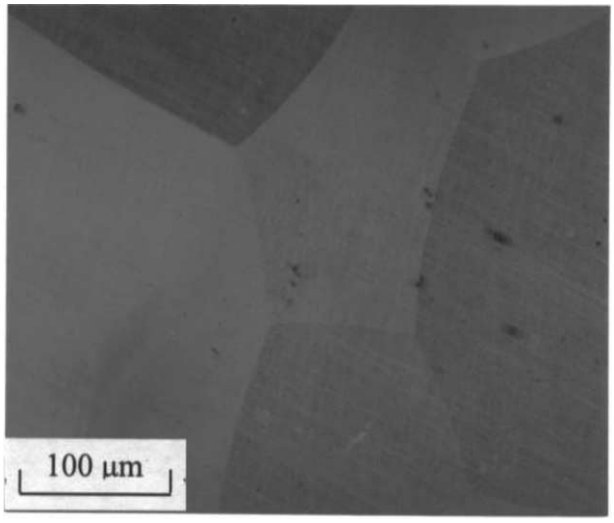

Fig. 1. An optical micrograph of the as-quenched alloy.

* Corresponding author. Tel.: +886-3-571-2121x55365; fax: +886-3-572-4727.

E-mail address: andychen.mse86g@nctu.edu.tw (C.H. Chen).

0921-5093/03/$ - see front matter © 2003 Elsevier Science B.V. All rights reserved.
doi:10.1016/S0921-5093(03)00041-8

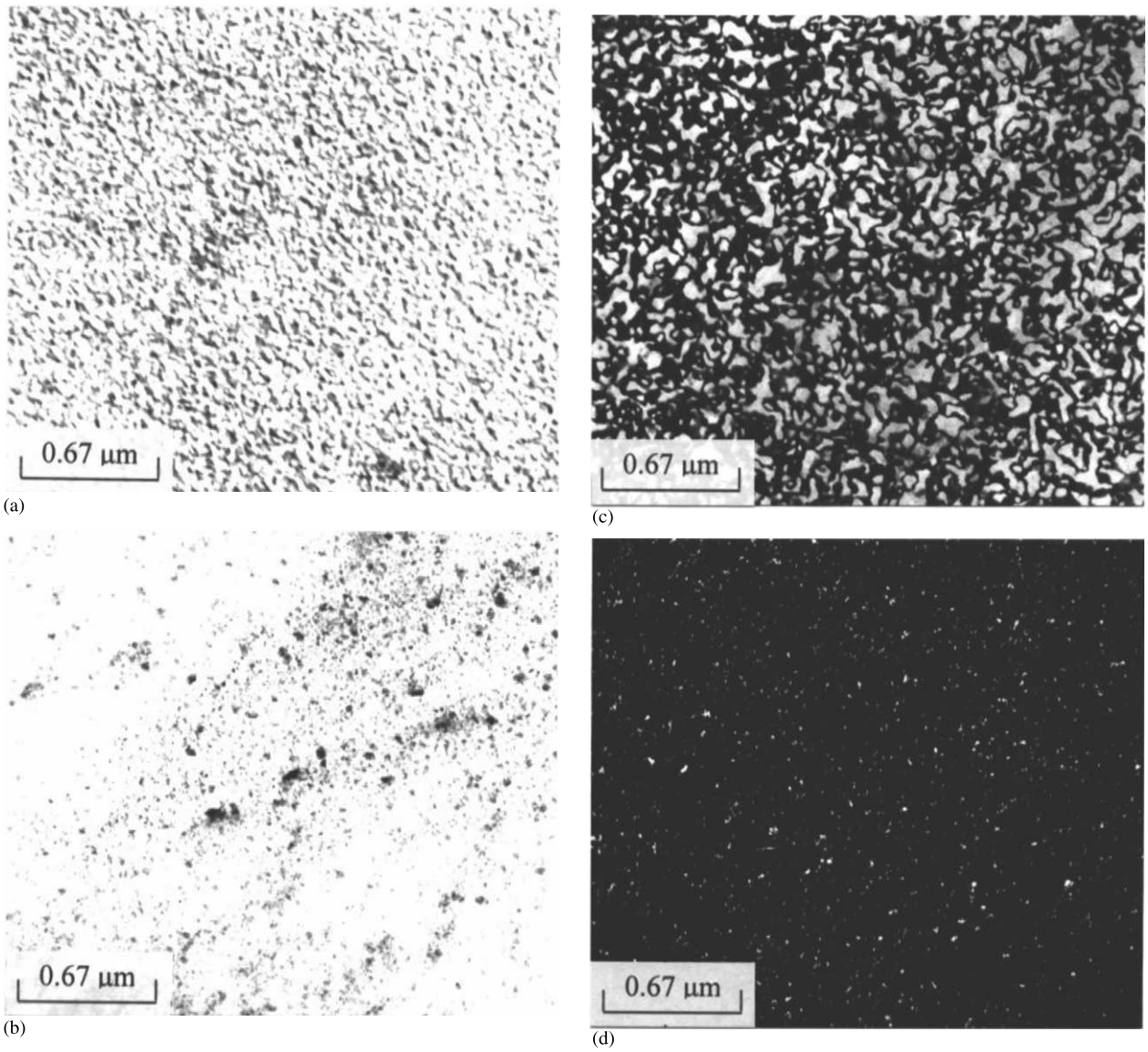

Fig. 2. Electron micrographs of the as-quenched alloy. (a) BF, (b) (002) $D0_3$, (c) ($\bar{1}11$) $D0_3$, and (d) an L-J DF, respectively.

To date, most examinations have focused on the Cu–Al–Ni alloys with Ni $\leqq$ 4.3 wt.% [1–12]. Little information concerning the aging effects of the Cu–Al binary alloy with a higher nickel content has been provided. Accordingly, the purpose of this study is an attempt to investigate the phase transition of the Cu–14.1 wt.% Al–9.0 wt.% Ni alloy using optical microscopy (OM), scanning electron microscopy (SEM), transmission electron microscopy (TEM) and energy-dispersive X-ray spectrometry (EDS). In the as-quenched condition, the microstructure of the alloy was $D0_3$ phase that contained extremely fine L-J precipitates, which was firstly found and identified by the authors in a $Cu_{2.2}Mn_{0.8}Al$ alloy [14]. Additionally, when the as-quenched alloy was aged at 500 °C for a long time, a phase transition $D0_3 \rightarrow D0_3 + B2 \rightarrow D0_3 + B2 + \alpha \rightarrow B2 + \alpha + \gamma_2$ occurred. This transition is quite different from that previously observed by other researchers in the aged Cu–Al–Ni alloys.

2. Experimental procedure

The alloy, Cu–14.1 wt.% Al–9.0 wt.% Ni, was prepared in a vacuum induction furnace using 99.9% copper, 99.9% aluminum and 99.9% nickel. The melt was chill cast into a $30 \times 50 \times 200$-mm copper mold. After being homogenized at 1000 °C for 72 h, the ingot was sectioned into 2.0-mm-thick slices. These slices were subsequently solution heat-treated at 1050 °C for 1 h and then quenched into iced-brine. Aging was performed at 500 °C for various times in a vacuum furnace.

Specimens for OM observations were prepared by sectioning, mounting, polishing and etching. The etch-

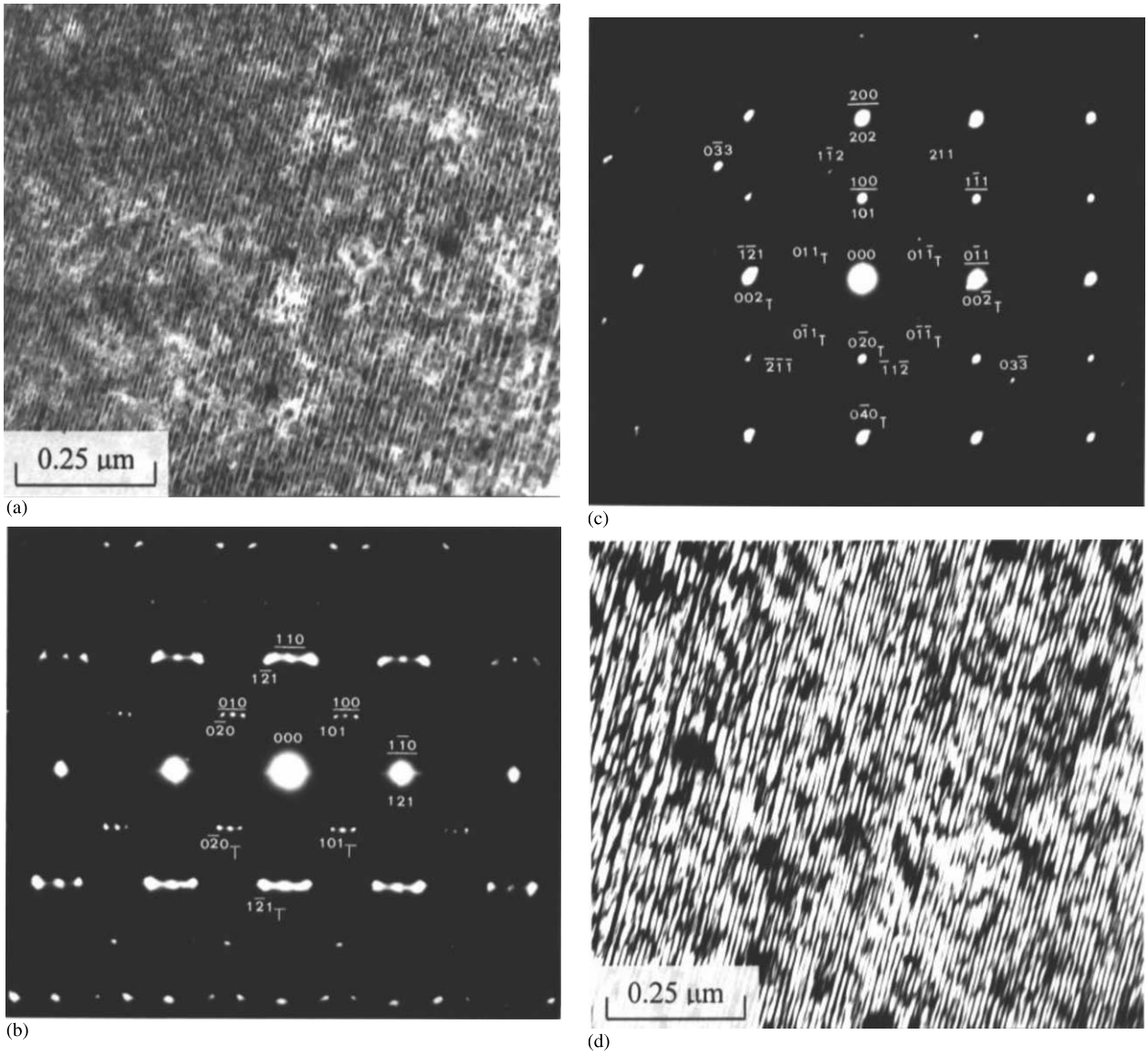

Fig. 3. Electron micrographs of the alloy aged at 500 °C for 10 min. (a) BF, (b) and (c) two SADPs. The zone axes of B2 phase, γ_1' martensite and internal twin are (b) [001], [10$\bar{1}$] and [$\bar{1}$01], and (c) [011], [1$\bar{1}\bar{1}$] and [$\bar{1}$00], respectively. (hkl = B2 phase, hkl = γ_1' martensite, hkl_T = internal twin). (d) and (e) (1$\bar{2}$1) γ_1' and $(100)_{B2}$ DF.

ing solution used was 25% nital solution (25 vol.% HNO_3 and balanced ethanol). Specimens for SEM were electrolytically etched in 30 vol.% nitric acid in methanol at −10 °C, using a potential of 5 V, after polishing. Thin foil specimens for TEM were prepared by means of a double-jet electropolisher with an electrolyte of 65 vol.% methanol and 35 vol.% nitric acid. The polishing temperature was maintained between −40 and −20 °C, and the current density was maintained between 3.0×10^4 and 4.0×10^4 A m^{-2}. Electron microscopy of thin foils was performed on a JEOL[1] JEM-2000FX scanning transmission electron microscope operating at 200 kV. This microscope was equipped with a Link ISIS 300 EDS for chemical analysis. The elemental concentrations of Cu, Al and Ni were quantitatively analyzed by the Cliff-Lorimer Ratio Thin Section method.

3. Results

Fig. 1 displays an optical micrograph of the present alloy after being solution heat-treated at 1050 °C for 1 h followed by quenching. The micrograph reveals a single-phase microstructure. However, the TEM examinations indicated that in the as-quenched condition, the microstructure of the alloy was $D0_3$ phase that contained extremely fine L-J precipitates. Fig. 2 presents a typical microstructure. This result is similar to that obtained by

[1] JEOL is a trademark of Japan Electron Optics Ltd., Tokyo.

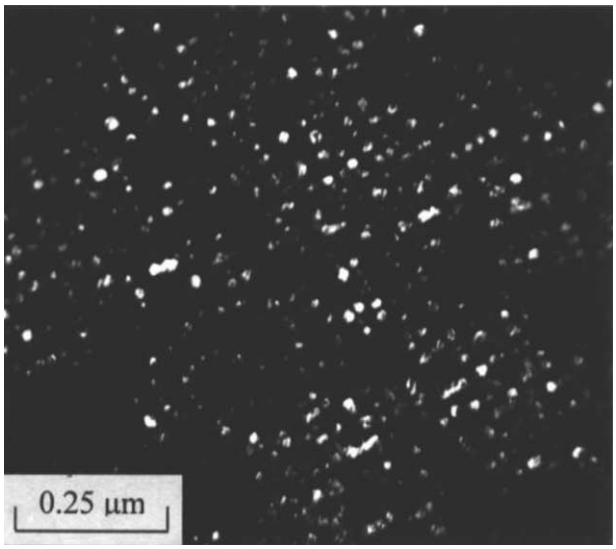

(e)

Fig. 3 (*Continued*)

the present workers in the Cu–14.6Al–4.3Ni (wt.%), Cu–14.2Al–xNi ($x = 4.3$, 6.0 and 10.0 wt.%), Cu_2MnAl and $Cu_{2.2}Mn_{0.8}Al$ alloys [12–15].

When the as-quenched alloy was aged at 500 °C for 10 min and then quenched into iced-brine, neither the $D0_3$ nor the L-J phase could be observed but an extremely thin lamellar structure could be seen, as illustrated in Fig. 3(a). Fig. 3(b) and (c), two selected-area diffraction patterns (SADPs) of the lamellar structure matrix, clearly indicate that these diffraction patterns consist of two sets of reflection reciprocal lattices. Following the results of previous studies of Cu–Al–Ni alloys [2,8,10], one set derived from the B2 phase, and another derived from the γ_1' martensite with internal twins. Fig. 3(d) and (e), $(1\bar{2}1)$ γ_1' and (100) B2 dark-field (DF) electron micrographs, clearly demonstrate the presence of the γ_1' martensite and the extremely fine B2 particles, respectively. In the previous studies [3,7,11], the investigators have proposed that when the Cu–14Al–4Ni (wt.%) alloy was aged at 450 °C for short times and then cooled to 160 °C or below, the $D0_3 \rightarrow \gamma_1'$ martensitic transformation occurred during cooling, and the increase of either aluminum or nickel content lowered the martensitic transformation temperature. The aluminum content of the alloy considered here is similar to that of Cu–14Al–4Ni (wt.%) alloy but the nickel content is apparently higher. Consequently, the γ_1' martensite presented in Fig. 3(a) can be concluded to have been formed through the $D0_3 \rightarrow \gamma_1'$ martensitic transformation during quenching from the aging temperature, rather than at the aging temperature. Accordingly, the microstructure of the alloy is a mixture of ($D0_3 + B2$) phases during the early stage of isothermal aging at 500 °C.

Fig. 4(a) shows an optical micrograph of the alloy aged at 500 °C for 1 h and then quenched, revealing that many numerous strip-like precipitates were formed within the matrix. Fig. 4(b) is a bright-field (BF) electron micrograph of the aged alloy, and shows the region that is contiguous to the interface between the strip-like precipitate and its surrounding matrix. Many granular and irregularly shaped particles were clearly formed within region A (matrix in Fig. 4(a)) and B (strip-like precipitate in Fig. 4(a)), respectively. Electron diffraction analyses demonstrated that both the granular and the irregularly shaped particles are of the B2 phase. Fig. 4(c) presents an SADP taken from the region A that contains the granular B2 particles and its surrounding matrix in Fig. 4(b). In this figure is the same as that in Fig. 3(b). From the characteristics of the lamellar structure and the associated SADP, it is seen that the region A of view corresponds to the γ_1' martensite containing B2 phase. Fig. 4(d), an SADP taken from the region B that covers the irregularly shaped B2 particle and its contiguous matrix in Fig. 4(b), reveals that the reflective spots correspond to the B2 phase, and other spots are of the α phase (a disordered face-centered cubic structure with lattice parameter $a = 0.327$ nm) [1]. Fig. 4(d) also shows that the orientation relationship between the irregularly shaped B2 particle and the disordered α phase was $(011)_{B2}//(111)_\alpha$ and $[1\bar{1}1]_{B2}//[10\bar{1}]_\alpha$, corresponding to the K–S orientation relationship [16]. Notably, the N–W orientation relationship between the B2 particle and the α phase was detected within another disordered α phase in the same specimen [16], as depicted in Fig. 4(e). Fig. 4(f) is a (100) B2 DF electron micrograph, clearly showing that the granular and the irregularly shaped

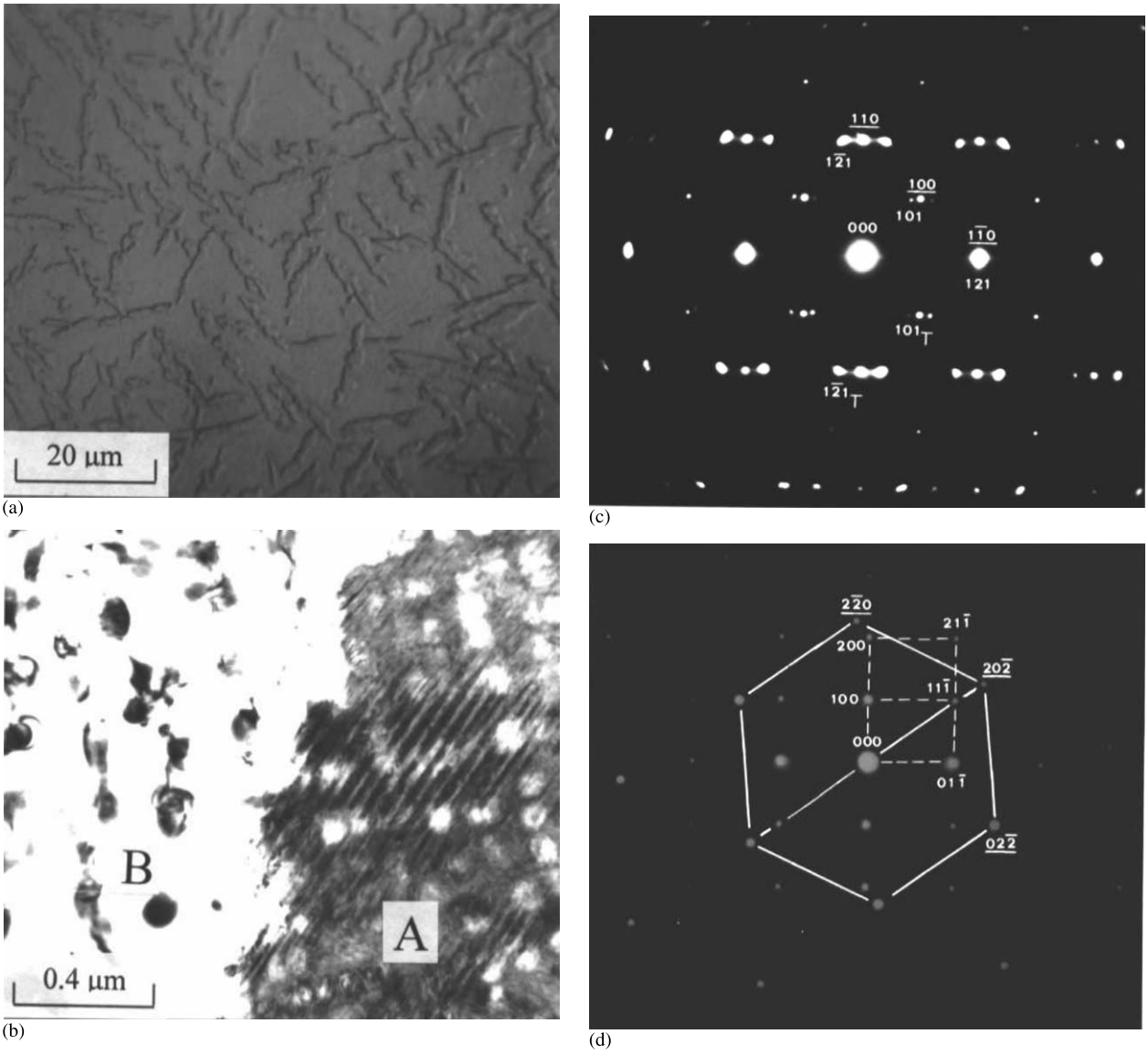

Fig. 4. Micrographs of the alloy aged at 500 °C for 1 h. (a) optical micrograph showing that the polycrystalline α phase with strip-like formed within the matrix, (b)-(f) electron micrographs, (b) BF, (c) an SADP taken from the region A containing the granular B2 particle and its surrounding matrix in (b), (d) an SADP taken from the region B covering the irregularly shaped B2 particle and its contiguous matrix in (b) showing the K–S orientation relationship between B2 particle and disordered α phase: $(110)_{B2}//(111)_{\alpha}$ and $[001]_{B2}//[0\bar{1}1]_{\alpha}$. (hkl = B2 phase, $\underline{hkl}$ = α phase). (e) an SADP showing the N–W orientation relationship between B2 particle and disordered α phase: $(100)_{B2}//(211)_{\alpha}$ and $[001]_{B2}//[0\bar{1}1]_{\alpha}$. (hkl = B2 phase, $\underline{hkl}$ = α phase). (f) (100) B2 DF.

B2 particles were formed within the γ_1' martensite and the disordered α phase, respectively.

Nevertheless, after prolonged aging at 500 °C, the polycrystalline α phase migrated and grew (light-etching areas) and the remaining $D0_3$ matrix was decomposed on the α/α interface (dark-etching contrast), as illustrated in Fig. 5(a). Fig. 5(b) shows an SEM micrograph magnified from the α/α interface that consists of light-etching disordered α matrix and the remaining $D0_3$ eutectoid decomposition product $\alpha+\gamma_2$ with a lamellar structure. However, the TEM examinations indicated that the B2 phase was still present after prolonged aging, and the size of the B2 phase was not increased apparently. Fig. 5(c) is a BF electron micrograph, displaying the area of the eutectoid ($\alpha+\gamma_2$) lamellar structure. Many irregularly shaped and granular particles were found within the eutectoid α and γ_2 phases, respectively. Fig. 5(d) and (e) show two SADPs taken from the region marked as "R" in Fig. 5(c). Analyses of the diffraction patterns confirmed that the precipitate had an ordered body-centered cubic structure with lattice parameter, $a = 0.872$ nm, which was consistent with that of the γ_2 phase [1,8]. In addition, the orientation relationship between the granular B2 particle and the eutectoid γ_2 phase is cubic to cubic. This finding is similar to that observed by other researchers

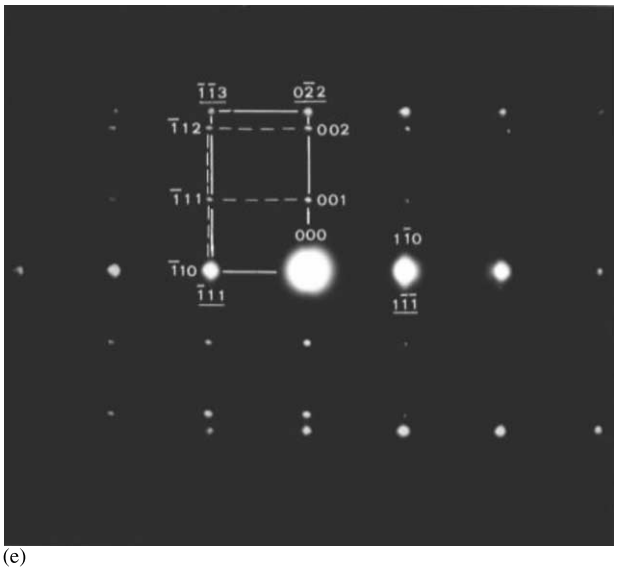

(e)

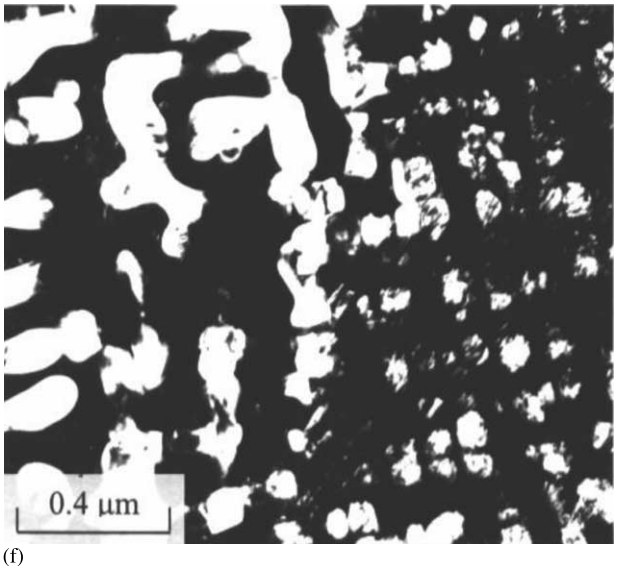

(f)

Fig. 4 (*Continued*)

in the aged Cu–Al–Ni alloys [10]. Fig. 5(f) presents a (100) B2 DF electron micrograph, which clearly reveals the presence of the B2 particles. Fig. 5(g) and (h) show that the orientation relationships between the B2 particle and the eutectoid α phase in regions, 'C' and 'D', were determined to be K–S and N–W orientation relationships, respectively [16].

4. Discussion

During the early stage of isothermal aging of the alloy at 500 °C, a high density of the extremely fine B2 particles was observed within the extremely thin lamellar γ_1' martensite, which was formed by the $D0_3 \rightarrow \gamma_1'$ martensitic transformation during quenching. The strip-like α phase was precipitated, and the size of B2 particles, especially those within the α phase, increased with the aging time increased at 500 °C, as shown in Fig. 4(a) and (b). After prolonged aging at 500 °C, the γ_1' martensite was eliminated and the remaining $D0_3$ matrix transformed to the $\alpha+\gamma_2$ phases via the eutectoid reaction. Therefore, the isothermal phase transition sequence was $D0_3 \rightarrow D0_3+B2 \rightarrow D0_3+B2+\alpha \rightarrow B2+\alpha+\gamma_2$ as the aging time increased at 500 °C. This finding is quite different from the $D0_3 \rightarrow D0_3+\gamma_2 \rightarrow \gamma_2+\alpha+\beta$ transition observed by other researchers in the Cu–14 Al–4 Ni (wt.%) alloy aged at 500 or 550 °C [7,9]. In order to elucidate the apparent difference and the characteristics of this isothermal transition of the alloy aged at 500 °C, a TEM-EDS study was undertaken. Fig. 6(a) through (e) represent five typical EDS spectra of the as-quenched specimen and the granular B2 particle (within the γ_1' martensite), the γ_1' martensite,

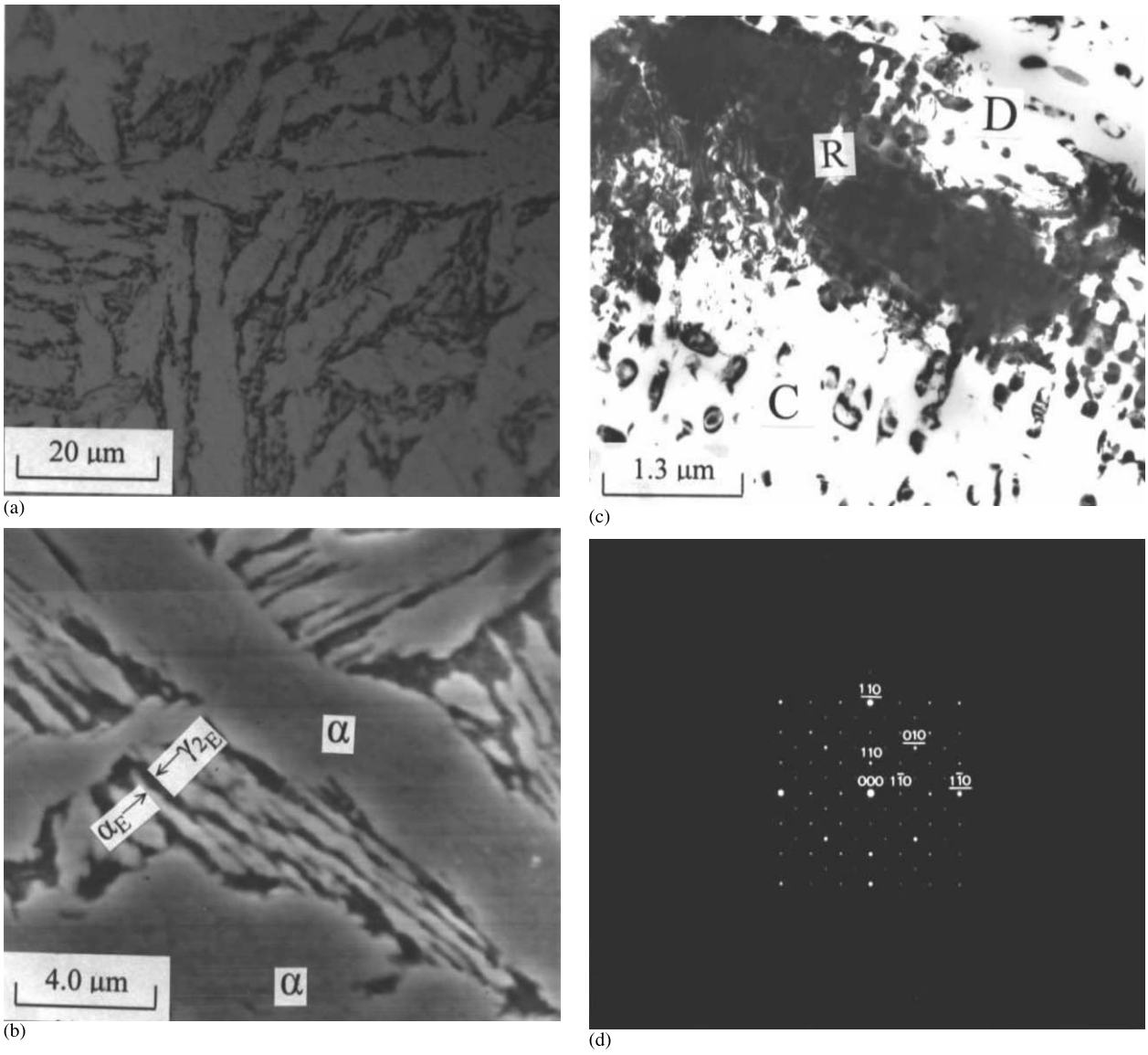

Fig. 5. Micrographs of the alloy aged at 500 °C for 20 h. (a) optical micrograph showing light-etching α phase and dark-etching $D0_3$ decomposition products, (b) SEM micrograph showing the microstructure in prior decomposed $D0_3$ region (α: polycrystalline α matrix; α_E: eutectoid α phase; γ_{2E}: eutectoid γ_2 phase), (c)-(h) electron micrographs, (c) BF, (d) and (e) 2 SADPs. The zone axes of the B2 particle and the eutectoid γ_2 phase are (d) [001] and [001] and (e) [011] and [011], respectively. (hkl = B2 phase, hkl = γ_2 phase). (f) (100) B2 *DF*, (g) and (h) 2 SADPs showing the K–S and N–W orientation relationships between the B2 particle and eutectoid α phase: $(11\bar{1})_{B2}//(10\bar{1})_\alpha$ and $[011]_{B2}//[111]_\alpha$, $(001)_{B2}//(0\bar{1}1)_\alpha$ and $[1\bar{1}0]_{B2}//[1\bar{1}\bar{1}]_\alpha$, respectively. (hkl = B2 phase, hkl = α phase).

the irregularly shaped B2 particle (within the disordered α phase), and the disordered α phase in the specimen aged at 500 °C for 1 h, respectively. Table 1 specifies the average weight percentages of the alloying elements obtained by analyzing at least ten different EDS spectra of each phase. For comparison, Table 1 also lists the chemical compositions of the B2, disordered α, eutectoid γ_2 and eutectoid α phases in the specimen aged at 500 °C for 20 h. The previous studies have proposed that the γ_2 phase would firstly form within the $D0_3$ matrix in the Cu–14Al–4Ni (wt.%) alloy aged at 500or 550 °C[7–9]. After increasing the aging time within this temperature range, the remaining $D0_3$ matrix was further transformed to (β+α). The nickel content of the alloy considered here greatly exceeds that of Cu–Al–Ni alloys investigated elsewhere. The authors' previous study demonstrated that adding nickel to an Fe–23.2 at.% Al alloy could pronouncedly enhance the formation of the B2 and B2* phases, of which the latter is also a B2-type phase and enriched in both aluminum and nickel [17]. Analogously and plausibly, adding much more nickel in the Cu–14.1 wt.% Al alloy should favor the formation of the B2 particles in the initial stage of aging at 500 °C. The EDS examinations revealed that along with the precipitation of the B2 particles, the aluminum and nickel content of the surrounding $D0_3$

matrix is predicted to decline since the aluminum and nickel concentrations in the B2 particles are very high. Previous studies have found that the concentration of aluminum in the γ_2 phase far exceeds that in the as-quenched alloy [7–10]. However, it is clearly seen in Table 1 that the aluminum concentration in the remaining $D0_3$ matrix (i.e. γ_1' martensite) is about 12.31 wt.%, which is less than that of the as-quenched alloy in the present study. It is, thus, reasonable to believe that due to the lower aluminum content in the remaining $D0_3$ matrix, it would disadvantage the precipitation of the Al-rich γ_2 phase in the initial aging stage and cause the $D0_3$ matrix to transform to the γ_1' martensite during quenching in the present alloy. In addition, the EDS examinations also showed that the chemical compositions of the B2 particles within the γ_1' martensite and the α phase are similar; however, the aluminum content of the γ_1' martensite is higher than that of the α phase. The polycrystalline α phase grew after the B2 particles reached an equilibrium concentration as the aging time increased. The α phase is suggested to reject the excess concentration of aluminum into the surrounding $D0_3$ matrix, and then the remaining $D0_3$ matrix is enriched in aluminum as the α interface advances. The enrichment of aluminum enhances the formation of the γ_2 phase in the regions contiguous to the α phase. Accordingly, after the grain boundaries of the polycrystalline α phases came across with each other, the sufficient aluminum content on the α/α interface is expected to promote that the $D0_3 \rightarrow \alpha + \gamma_2$ eutectoid reaction occurred.

Finally, it is worthy to point out that no evidence of the γ_1' martensite plates was detected using OM, as shown in Fig. 4(a). In fact, Fig. 4(b) clearly shows the lamellar γ_1' martensite. The high density of the extremely

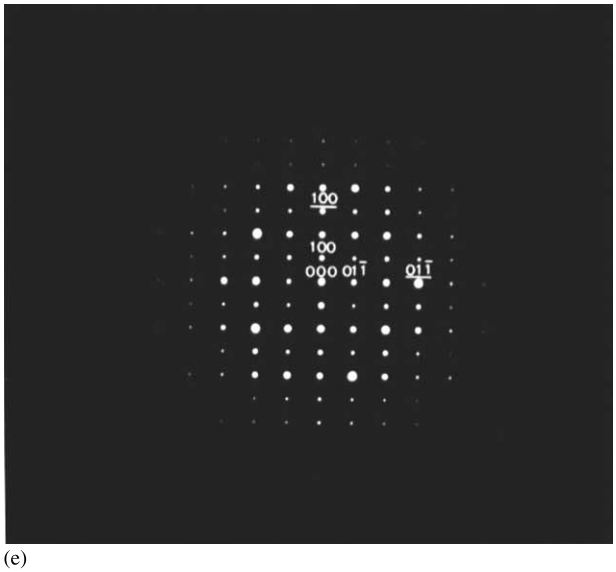

(e)

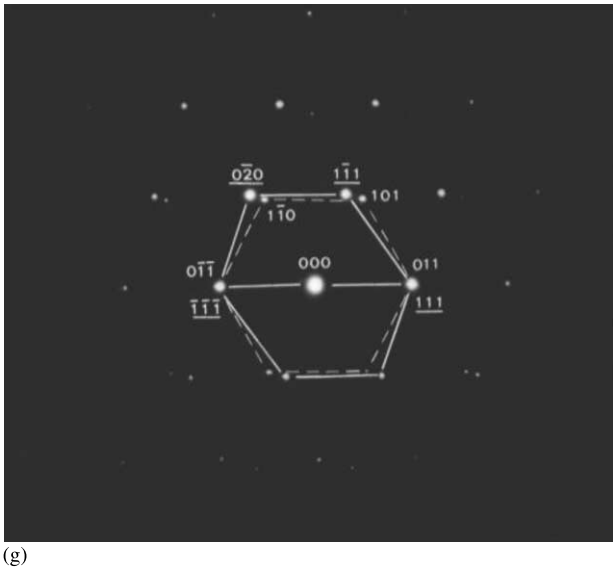

(g)

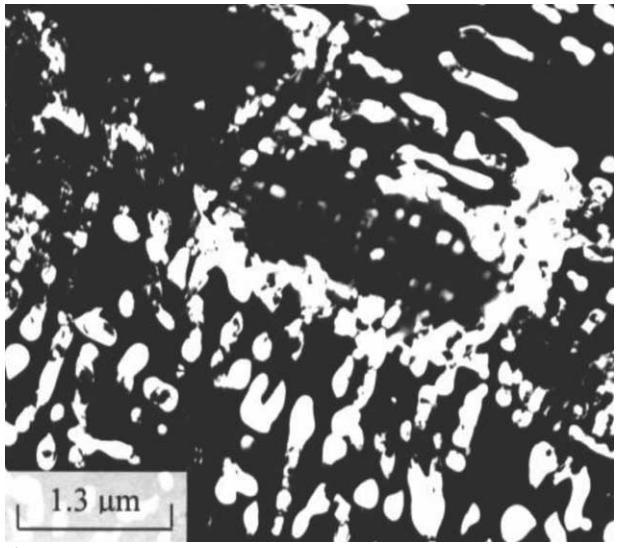

(f)

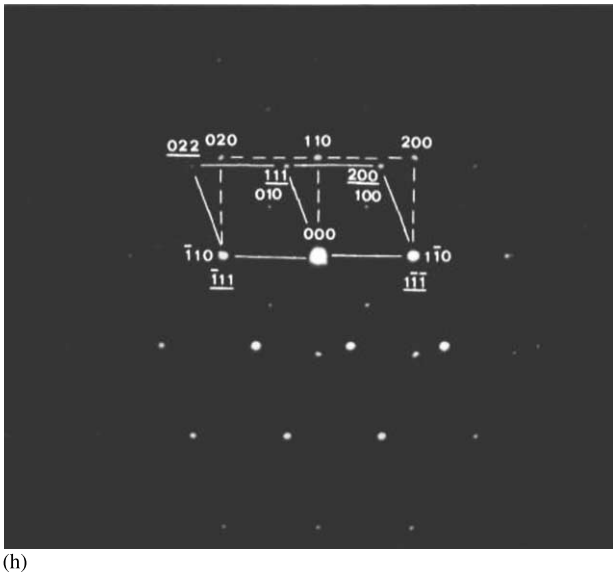

(h)

Fig. 5 (*Continued*)

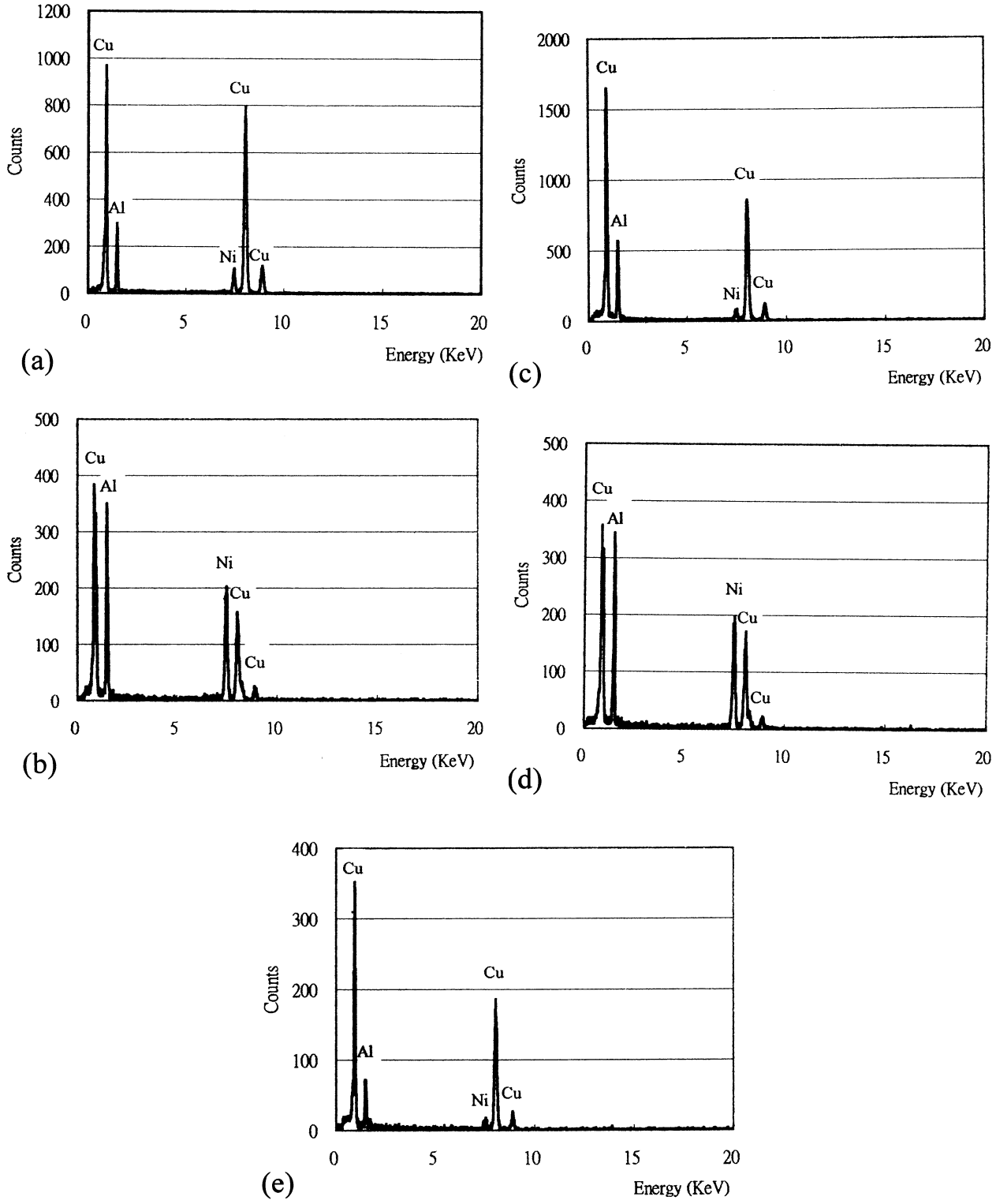

Fig. 6. Five typical EDS spectra obtained from (a) as-quenched alloy, and (b) a B2 particle within the γ_1' martensite, (c) a γ_1' martensite, (d) a B2 particle within the disordered α phase as well as (e) a disordered α phase in the alloy aged at 500 °C for 1 h.

fine B2 particles can thus be reasonably suggested to restrict the γ_1' martensite to form an extremely thin lamellar structure with short segments, preventing any large γ_1' martensite plate from being examined. This resembles the result of Kuwano et al. [2].

Table 1
Chemical compositions of the phases revealed by an energy-dispersive X-ray spectrometer (EDS)

Heat treatment	Phase	Chemical composition (wt pct)		
		Cu	Al	Ni
As-quenched	$D0_3$+L-J	76.86±0.6	14.13±0.6	9.01±0.3
500 °C 1 h	B2 phase (within γ_1' martensite)	36.47±0.7	23.97±0.6	39.56±0.4
	γ_1' martensite (i.e. the remaining $D0_3$ matrix)	80.97±0.5	12.31±0.5	6.72±0.4
	B2 phase (within disordered α phase)	37.12±0.8	22.85±0.5	40.03±0.5
	Disordered α phase	86.19±0.4	9.68±0.5	4.13±0.4
500 °C 20 h	Disordered α phase	91.71±0.6	6.40±0.5	1.89±0.2
	B2 phase (within eutectoid γ_2 phase)	24.99±0.7	29.34±0.6	45.67±0.6
	Eutectoid γ_2 phase	78.45±0.6	14.51±0.6	7.04±0.4
	B2 phase(within eutectoid α phase)	12.88±0.6	31.52±0.7	55.60±0.4
	Eutectoid α phase	89.94±0.6	7.87±0.4	2.19±0.6

5. Conclusions

On the basis of the above experimental results, the phase transition in the Cu–14.1 wt.% Al–9.0 wt.% Ni alloy could be summarized as follows:

1) The as-quenched microstructure of the alloy is a mixture of ($D0_3$+L-J) phases.
2) The higher nickel content in the Cu–Al–Ni alloy would enhance the precipitation of the B2 particles but disadvantage the formation of the γ_2 phase in the initial aging stage.
3) With increasing the aging time at 500 °C, the phase transition sequence was found to be $D0_3 \rightarrow D0_3 + B2 \rightarrow D0_3 + B2 + \alpha \rightarrow B2 + \alpha + \gamma_2$.
4) Both K–S and N–W orientation relationships between the B2 particle and the disordered α matrix or the eutectoid α phase could be detected in the aged alloy.

Acknowledgements

The authors are pleased to acknowledge the financial support of this research by the National Science Council, Republic of China under Grant NSC90-2216-E-009-044. They are also grateful to M.H. Lin for typing.

References

[1] M.A. Dvorack, N. Kuwano, S. Polat, H. Chen, C.M. Wayman, Scripta Metall. 17 (1983) 1333–1336.
[2] N. Kuwano, C.M. Wayman, Metall. Trans. 15A (1984) 621–626.
[3] N.F. Kennon, D.P. Dunne, L. Middleton, Metall. Trans. 13A (1982) 551–555.
[4] N. Zárubová, A. Gemperle, V. Novák, Mater. Sci. Eng. A222 (1997) 166–174.
[5] K. Otsuka, H. Sakamoto, K. Shimizu, Trans. JIM 20 (1979) 244–254.
[6] K. Otsuka, H. Kubo, C.M. Wayman, Metall. Trans. 12A (1981) 595–605.
[7] J. Singh, H. Chen, C.M. Wayman, Metall. Trans. 17A (1986) 65–72.
[8] J. Singh, H. Chen, C.M. Wayman, Scripta Metall. 19 (1985) 887–890.
[9] J. Singh, H. Chen, C.M. Wayman, Scripta Metall. 19 (1985) 231–234.
[10] Y.S. Sun, G.W. Lorimer, N. Ridley, Metall. Trans. 21A (1990) 575–588.
[11] V. Agafonov, P. Naudot, A. Dubertret, B. Dubois, Scripta Metall. 22 (1988) 489–494.
[12] J. Tan, T.F. Liu, Mater. Chem. Phys. 70 (2001) 49–53.
[13] J. Tan, T.F. Liu, Scripta Mater. 43 (2000) 1083–1088.
[14] S.C. Jeng, T.F. Liu, Metall. Trans. 26A (1995) 1353–1365.
[15] K.C. Chu, T.F. Liu, Metall. Trans. 30A (1999) 1705–1716.
[16] J.W. Edington, Electron Diffraction in the Electron Microscope, vol. 2, The MacMillan Press, London, 1975, pp. 116–117.
[17] T.F. Liu, S.C. Jeng, C.C. Wu, Metall. Trans. 23A (1992) 1395–1401.